RC: We thank the reviewer for reading the manuscript and for providing feedback to improve the paper. We address each individual comment below, and we included a file tracking the changes to the manuscript at the end of this document*.*

General comments:

The authors implemented six different improvements to WRF-Chem 3.5.1 in order to increase the simulation quality in the Arctic: a correction to the sedimentation of aerosol particles, emissions and gas-phase chemistry of DMS, improved representation of the dry deposition over seasonal snow, UV-albedo dependence on snow and ice cover for photolysis calculations, better representation of surface temperatures over melting ice in the Noah Land Surface Model, and a cumulus parameterization that includes the effect of cumulus clouds on aerosol and trace gas concentration. The effect of each of these improvements on simulated ozone and aerosol concentrations is discussed in the paper and compared against observations. In total, the paper describes excellent work, which contributes significantly to the development of WRF-Chem and to the comprehension of processes which affect air pollution in the Arctic region.

RC: We thank the reviewer for these comments.

Minor comments:

COMMENT 1: Page 4, line 15: Please mention the projection
RC: The simulation domain is on a polar stereographic projection. This is now mentioned in the text, p. 4 l. 10.

COMMENT 2: Page 7, lines 14-20: Please add some more details about the implementation of secondary Activation
RC: The version of KF-CuP used in this study includes secondary activation of aerosols above the cloud base, which was not included in Berg et al. (2015), and primary activation at cloud base. For primary activation, the model calculates the maximum supersaturation using the Abdul-Razzak and Ghan (2000) parameterization with the cloud-base updraft speeds from the KF-CuP parameterization and the simulated aerosol concentrations in the updrafts. Secondary activation assumes a fixed maximum supersaturation of 0.1%. Aerosol activation is then calculated from the maximum supersaturations and the critical supersaturations for each aerosol size bin. We now give these details in the text, p 7, ll. 14-19.

Abdul-Razzak, H. and Ghan, S. J.: A parameterization of aerosol activation: 2. Multiple aerosol types, J. Geophys. Res.-Atmos., 105, 6837–6844, 2000.

COMMENT 3: Page 15, last line: This is an important result, which should be emphasized and discussed in more detail and also be addressed in the conclusions.
RC: We added more details in the text, p. 16 ll. 2-7:
"… indicating that these processes should also be taken into account when studying ozone at lower latitudes with WRF-Chem. At subarctic sites (latitude < 60 N), model updates decrease RMSE by 13 % on average, and by more than 50 % at 9 surface sites. These improvements in

the midlatitudes are mostly due to the KFCUP_CHEM update, and to the SNOWDEP_SNOWPHOT update at sites where seasonal snow is present. Ahmadov et al. (2015), using WRF-Chem 3.5.1 , also showed that reduced deposition and enhanced photolysis over snow could contribute to high wintertime ozone in the United States when other favorable conditions were present, such as shallow boundary layers and high emissions."
We now also address this in the conclusions, p. 18, ll.14-21.

COMMENT 4: Correlations should be discussed more extensively besides the RMSE.
RC: We now give the correlations between model results and the different datasets, and discuss them in the text, p. 13, ll.8-9, p. 14, ll. 6-7 and 15-16, and p. 15 ll. 13-14. For surface BC, the average Pearson correlation coefficient increases from 0.43 to 0.87 in the updated model, and from 0.28 to 0.73 for SO_4, due to the improved representation of the seasonal cycle of aerosols at the Arctic surface. For ARCTAS BC, the correlation coefficient before model updates is very low in spring (0.07) and low in summer (0.48), and changes very little with the updates (0.08 and 0.43 respectively), since both versions of the model do not reproduce the observed vertical structure of BC pollution in the Arctic troposphere.

COMMENT 5: The authors might consider an extension of the conclusions in order to keep up with the overall high quality of the paper and to enhance the readability of the second paragraph (just a suggestion how, no condition for acceptance of the paper).
RC: We updated the conclusions to improve their readability, especially p. 18, ll. 5-21.

Improvements to the WRF-Chem 3.5.1 model for quasi-hemispheric simulations of aerosols and ozone in the Arctic

Louis Marelle[1,2,a], Jean-Christophe Raut[1], Kathy S. Law[1], Larry K. Berg[3], Jerome D. Fast[3], Richard C. Easter[3], Manish Shrivastava[3], and Jennie L. Thomas[1]

[1]LATMOS/IPSL, UPMC Univ. Paris 06 Sorbonne Universités, UVSQ, CNRS, Paris, France
[2]TOTAL S.A, Direction Scientifique, Tour Michelet, 92069 Paris La Défense, France
[3]Pacific Northwest National Laboratory, Richland, WA, USA
[a]Now at: Center for International Climate and Environmental Research, Oslo, Norway

Correspondence to: Louis Marelle (louis.marelle@cicero.oslo.no)

Abstract. In this study, the WRF-Chem regional model is updated to improve simulated short-lived pollutants (aerosols, ozone) in the Arctic. Specifically, we include in WRF-Chem 3.5.1 (with SAPRC-99 gas-phase chemistry and MOSAIC aerosols) (1) a correction to the sedimentation of aerosols, (2) dimethylsulfide (DMS) oceanic emissions and gas-phase chemistry, (3) an improved representation of the dry deposition of trace gases over seasonal snow, (4) an UV-albedo dependence on snow and ice cover for photolysis calculations. We also (5) correct the representation of surface temperatures over melting ice in the Noah Land Surface Model and (6) couple and further test the recent KF-CuP (Kain-Fritsch + Cumulus Potential) cumulus parameterization that includes the effect of cumulus clouds on aerosols and trace gases. The updated model is used to perform quasi-hemispheric simulations of aerosols and ozone, which are evaluated against surface measurements of black carbon (BC), sulfate, and ozone, and airborne measurements of BC in the Arctic. The updated model shows significant improvements in terms of seasonal aerosol cycles at the surface, root mean square errors (RMSE) for surface ozone and aerosols and BC aloft, compared to the base version of the model and to previous large-scale evaluations of WRF-Chem in the Arctic. These improvements are mostly due to the inclusion of cumulus effects on aerosols and trace gases in KF-CuP (improved RMSE for surface BC and BC profiles, surface sulfate and surface ozone), the improved surface temperatures over sea ice (surface ozone, BC, and sulfate), and the updated trace gas deposition and UV-albedo over snow and ice (improved RMSE and correlation for surface ozone). DMS emissions and chemistry improve surface sulfate at all Arctic sites except Zeppelin, and correcting aerosol sedimentation has little influence on aerosols except in the upper troposphere.

1 Introduction

The Arctic is one of the the fastest warming regions on Earth (IPCC, 2013). Early studies have shown that 20th century Arctic warming was mostly a consequence of the increased concentration of well-mixed greenhouse gases (e.g. CO_2 and CH_4), associated with the effect of shorter-lived climate forcers, especially aerosols and ozone (Shindell et al., 2006). As a result, mitigating Arctic warming requires first and foremost global reductions of carbon emissions. However, controlling short-lived species could be a faster and more cost-effective way to limit Arctic and global warming, while also improving air quality (e.g., Stohl et al., 2015), since aerosols and ozone are also harmful air pollutants.

Global climate and chemistry-transport models are key tools used to understand the past and future roles of short-lived pollutants. However, modeling aerosol and ozone pollution in the Arctic has proven very challenging in the past. Studies by Shindell et al. (2008), Koch et al. (2009) and Schwarz et al. (2010) have shown that most models at the time strongly underestimated black carbon (BC) observed at the Arctic surface, and overestimated it aloft. In addition, models often failed to reproduce the observed seasonal cycle of surface aerosol pollution, which peaks in late winter and early spring due to enhanced transport from the midlatitudes and lower deposition efficiencies (Quinn et al., 2007). Studies have since showed that these model biases were likely caused by the limited horizontal resolution (Sato et al., 2016; Raut et al., 2017), missing local emission sources (Stohl et al., 2013), and poorly known removal processes. Specifically, Huang et al. (2010), Liu et al. (2012), Browse et al. (2012), Wang et al. (2013) showed that Arctic BC could be improved by the use of more complex aerosol wet removal schemes within models. However, implementing these schemes does not fully resolve model disagreement with BC measurements (Browse et al., 2012; Wang et al., 2014; Eckhardt et al., 2015; Schwarz et al., 2017), and recent research (Mahmood et al., 2016) indicates that differences in wet scavenging efficiencies are still the main cause of differences in Arctic BC burdens between models.

Concerning ozone, Emmons et al. (2015), Monks et al. (2015), and Arnold et al. (2015) showed that most models exhibit strong biases in ozone precursors such as nitrogen oxides ($\mathrm{NO_x}$), carbon monoxide (CO), peroxyacetyl nitrate (PAN) and several oxygenated Volatile Organic Compounds (VOCs), and underestimate ozone in the middle and high Arctic troposphere by ~ 10 to $30\ \%$. Similarly, results from the AMAP (2015) model intercomparison indicate that models are strongly biased in the Arctic for both ozone and its precursors. These biases are attributed to uncertainties in emissions, pollution transport and processing, overestimated stratosphere-troposphere exchange and uncertainties related to the hydroxyl radical OH.

The main known causes of model error in the Arctic (except emissions) can in theory be addressed by using regional models, for which global coverage can be traded for increased process complexity and higher resolutions. Several recent case studies have shown the validity of this approach, by using the regional WRF-Chem model (Weather Research and Forecasting model, including chemistry, (Grell et al., 2005; Fast et al., 2006) in order to understand the effect of local pollutant emissions from shipping at high latitudes (Mölders et al., 2010; Marelle et al., 2016), and the mechanisms of pollution transport from the midlatitudes to the Arctic (Sessions et al., 2011; Thomas et al., 2013; Marelle et al., 2015; Raut et al., 2017). However, these case studies were based on short, relatively local simulations, while Arctic pollution transported from the mid-latitudes can only be studied using long, quasi-hemispheric simulations, which can resolve both remote and local sources of Arctic pollution. Such a quasi-hemispheric WRF-Chem simulation was performed for the first time and evaluated in the intercomparisons of Eckhardt et al. (2015) and AMAP (2015). Unfortunately, in spite of its good performance for local case studies, WRF-Chem performed poorly in terms of aerosols (Eckhardt et al., 2015), failing to reproduce observed aerosol concentrations and their seasonal evolution in spring and summer 2008. AMAP (2015) showed that WRF-Chem performs reasonably well for ozone, but other research (Ahmadov et al., 2015) indicates that the version of WRF-Chem used in AMAP (2015) can be strongly biased low for ozone over snow-covered ground due to overestimated dry deposition and underestimated photolysis rates. In this context, the main objectives of this study are to improve WRF-Chem results for Arctic aerosols and ozone compared to the previous large scale model intercomparisons of Eckhardt et al. (2015) and AMAP (2015), to identify potential areas of further improvements in the WRF-Chem model, and to define a model setup that can be used in future work to study aerosol and ozone pollution at continental scales in the Arctic, defined in this study as the region north of 60° N.

The model setup and emissions are presented in Sect. 2. Section 3 presents how the WRF-Chem 3.5.1 model was updated for this study. The effect of these updates on Arctic aerosols and ozone is evaluated in Sect. 4, where results are also validated against surface and airborne measurements in the Arctic. Conclusions are presented in Sect. 5.

2 WRF-Chem

WRF-Chem (Grell et al., 2005; Fast et al., 2006) is a regional meteorological, chemistry, and aerosol model based on the mesoscale meteorological model WRF-ARW (Advanced Research WRF, Skamarock et al., 2008). WRF-Chem is fully integrated within WRF, and uses the same grid, time step, advection scheme and physics schemes as WRF. The developments presented in this study (presented in Sect. 3) are based on the version 3.5.1 of the model (the current version in March 2017 is 3.8.1 and does not include all but 2 of the updates presented here, Sect. 3). The version used here also includes the additions to WRF-Chem 3.5.1 related to the KF-CuP cumulus scheme and described in Berg et al. (2013) and Berg et al. (2015).

2.1 Model setup, domain and simulation period

The model setup is presented in Table 1. Briefly, the gas-phase chemistry mechanism is SAPRC-99 (Statewide Air Pollution Research Center, 1999 version; Carter, 2000). Photolysis rates used in the gas-phase chemistry calculations are calculated by the Fast-J scheme (Wild et al., 2000). Aerosols are represented by the MOSAIC (Model for Simulating Aerosol Interactions and Chemistry, Zaveri et al., 2008) model, with eight size bins between $39\,\mathrm{nm}$ and $10\,\mu\mathrm{m}$. The version of the SAPRC-99/MOSAIC-8bin mechanism used here includes bulk aqueous chemistry, as well as secondary organic aerosol (SOA) formation represented by the VBS-2 (Volatility Basis Set with 2 volatility species, Shrivastava et al., 2011) scheme, treating the partitioning of organic aerosols between the volatile and the condensed phase using the “volatility basis set” approach (Robinson et al., 2007). In this study, VBS-2 only includes SOA formation from the oxidation of anthropogenic and biogenic VOCs. SOA formation from Semi-volatile and Intermediate-Volatility Organic Compounds (S/IVOCs) was not included due to its high computational cost and due to the lack of accurate global S/IVOC emission inventories.

The MYJ (Mellor-Yamada-Janjić) scheme is used to represent the planetary boundary layer, with the associated Janjić Eta surface layer scheme (Janjić, 1994). The land surface is represented using Noah-LSM (unified Noah Land-Surface Model; Chen and Dudhia, 2001). Radiative calculations are performed using the RRTMG scheme (Rapid Radiative Transfer Model for Global applications; Iacono et al., 2008), which is coupled here with WRF-Chem predicted ozone and aerosol optical properties. The recommended microphysical scheme to be used with MOSAIC is the Morrison 2-moment scheme (Morrison et al., 2009). The Morrison 2-moment scheme calculates cloud formation, cloud properties, and precipitation at the grid scale, as well as aerosol activation in clouds, aqueous chemistry for activated aerosols, and wet removal. Subgrid clouds are represented using

Table 1. WRF-Chem 3.5.1 setup.

Option name	Selected option
Chemistry & aerosol options	
Gas-phase chemistry	SAPRC-99 (Carter, 2000)
Aerosols	MOSAIC 8-bins (Zaveri et al., 2008) + VBS-2 SOA formation and aqueous chemistry
Photolysis	Fast-J (Wild et al., 2000)
Metrorological options	
Planetary boundary layer	MYJ (Janjić, 1994)
Surface layer	Monin-Obukhov Janjic Eta scheme (Janjić, 1994)
Land surface	Unified Noah land-surface model (Chen and Dudhia, 2001)
Microphysics	Morrison (Morrison et al., 2009)
SW radiation	RRTMG (Iacono et al., 2008)
LW radiation	RRTMG (Iacono et al., 2008)
Cumulus parameterization	KF-CuP (Berg et al., 2015)

the KF-CuP (Kain-Fritsch + Cumulus Potential) parameterization developped by Berg et al. (2013). KF-CuP is a convective parameterization based on the Kain-Fritsch (Kain and Fritsch, 1990; Kain, 2004) cumulus scheme and the cumulus potential (Berg and Stull, 2005) scheme. The version of KF-CuP implemented in WRF-Chem (Berg et al., 2015) also represents the effect of cumulus clouds on aerosols and trace gases (additional details are given in Sect. 3.1).

Initial and boundary conditions for meteorology, as well as sea-surface temperatures (SST) and sea-ice, are specified using NCEP FNL (National Center for Environmental Prediction, final analysis); boundary conditions, SSTs and sea-ice are updated every $6\ \mathrm{h}$. In addition, WRF-Chem winds, temperature and humidity are nudged to the FNL analysis in the free troposphere (grid nudging) with the same $6\ \mathrm{h}$ update time. Initial and boundary conditions for chemistry are taken from the global model MOZART-4 (Model for Ozone and Related chemical Tracers; Emmons et al., 2010), and also updated every $6\ \mathrm{h}$. The simulation domain (polar stereographic projection) is presented in Fig. 1. It includes remote sources of pollution potentially transported to the Arctic in less than 30 days (Stohl, 2006), a transport time larger than the mean ozone and aerosol lifetimes in the troposphere (respectively 22 days and less than 10 days). Simulations are performed for the period from 1 March to 1 August 2008, in order to include both a period with active long-range pollution transport to the Arctic (March to early May) and a period when pollution removal processes are more prevalent (late May to July). The month of March is discarded as spin-up. In order to be computationally feasible, simulations are run at a relatively low horizontal resolution of ($100\ \mathrm{km} \times 100\ \mathrm{km}$), which is however 2 to 3 times finer than the typical resolutions used by most global models investigating Arctic aerosol and ozone (Eckhardt et al., 2015; Emmons et al., 2015). Simulations are performed for the year 2008, when many measurement

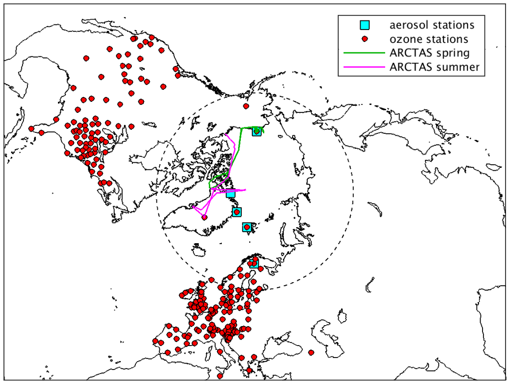

Figure 1. WRF-Chem simulation domain, and location of the measurements used in this study. Stations measuring ozone are shown as red circles. Arctic aerosol measurement sites (BC and sulfate) are shown as blue squares. ARCTAS spring and summer flight tracks north of 70° N (as in Eckhardt et al., 2015) are shown in green and pink, respectively.

datasets are available as part of the POLARCAT (Polar Study using Aircraft, Remote Sensing, Surface Measurements and Models, Climate, Chemistry, Aerosols and Transport, Law et al., 2014) project, and to allow comparison with the WRF-Chem simulation presented in Eckhardt et al. (2015) and AMAP (2015).

2.2 Emissions

Anthropogenic emissions are from the ECLIPSEv5 dataset (Evaluating the Climate and Air Quality Impacts of Short-Lived Pollutants, Klimont et al., 2016), except shipping emissions from RCP8.5 (Representative Concentration Pathway, Riahi et al., 2011). The ECLIPSEv5 inventory includes BC emissions from gas flaring in the Russian Arctic, which have been shown to improve the representation of Arctic BC by Stohl et al. (2013). Fire emissions are from FINNv1.5 (Fire INventory from NCAR, Version 1.5, Wiedinmyer et al., 2014). Soil NO emissions are from the POLMIP (POLARCAT Model Intercomparison Project) inventory (Emmons et al., 2015). Biogenic emissions from vegetation are calculated online by the MEGAN model (Model of Emissions of Gases and Aerosols from Nature, Guenther et al., 2006). Other emissions calculated online by the WRF-Chem model include sea salt, mineral dust (both from the GOCART model, Chin et al., 2002), and lightning $\mathrm{NO_x}$ emissions (Wong et al., 2013).

3 Improvements included in WRF-Chem 3.5.1

We identify several processes previously missing from the WRF-Chem model version 3.5.1 and potentially important for the representation of Arctic aerosols and ozone. This section presents the model updates included and evaluated in this study. (1) We include the effect of cumulus on aerosols and trace gases as represented in the KF-CuP cumulus scheme within WRF-Chem (Sect. 3.1). KF-CuP is used here, but it was included in WRF-Chem 3.5.1 in Berg et al. (2013) and Berg et al. (2015), and

Table 2. Simulation list and description.

Simulation name	Description
ALL_UPDATES	All model updates included
NO_KFCUP_CHEM	No effect of cumulus on aerosols and trace gases in the KF-CuP scheme
NO_SEDIMENTATION	No aerosol sedimentation above the first model level
NO_DMS	No dimethylsulfide (DMS) emissions or gas-phase chemistry
NO_SNOWDEP	No reduced dry deposition of gases over snow (March–April only)
NO_SNOWPHOT	No increased UV-albedo over snow and ice (March–April only)
NO_SNOWDEP_SNOWPHOT	Combination of NO_SNOWDEP and NO_SNOWPHOT (March–July)
NO_NOAH_SEAICE	No heat sink from melting sea-ice in Noah-LSM
NO_UPDATES	All updates above turned off

released in later WRF-Chem versions; it is here further coupled to other components of the model and its impacts on Arctic aerosols and ozone are evaluated. Updates developped specifically for this study include (2) the addition of sedimentation aloft in the MOSAIC aerosol model (Sect. 3.2); (3) the inclusion of DMS emissions and gas-phase chemistry in the SAPRC-99 gas-phase mechanism (Sect. 3.3), (4) the coupling of WRF snow to the dry deposition scheme (Sect. 3.4), (5) the inclusion of a dependence of UV-albedo on snow and ice cover in the Fast-J photolysis scheme (Sect. 3.5); and (6) the added heat sink from melting sea ice in calculations of the surface energy budget in the Noah-LSM surface model (Sect. 3.6). The updates presented in this section, except the KF-CuP scheme and the corrections to the Noah-LSM module, are not yet included in the latest version of WRF-Chem (3.8.1).

The different simulations performed to evaluate these updates are presented in Table 2. ALL_UPDATES is the reference simulation with all updates implemented, and NO_UPDATES a simulation where all updates presented in this section are turned off. We also perform simulations where each update is removed, leaving all of the others switched on (e.g., NO_SEDIMENTATION). The NO_KFCUP_CHEM simulation does not disable the KF-CuP cumulus scheme entirely, but only its impacts on trace gases and aerosols (aerosol activation, aqueous chemistry, tracer transport, wet removal). Due to limited computational resources, the updates related to deposition and photolysis over snow are only evaluated separately (i.e. NO_SNOWDEP and NO_SNOWPHOT) for the months of March and April, when snow cover is highest, but are evaluated together (i.e. NO_SNOWDEP_SNOWPHOT) for the full study period (March–July).

This section presents these previously missing processes in more detail, their relevance to Arctic short-lived pollutants, and how they were taken into account in the WRF-Chem 3.5.1 model. The effect of these changes on Arctic aerosols and ozone are evaluated and discussed in Sect. 4.

3.1 KF-CuP cumulus scheme and its effects on aerosols and trace gases

Aerosol/cloud and trace gas/cloud interactions in the MOSAIC aerosol model, including wet removal and aqueous chemistry, were previously only represented in WRF-Chem for grid-scale (resolved) clouds, but not for cumulus (parameterized) clouds. Berg et al. (2015) recently included the KF-CuP cumulus scheme in WRF-Chem 3.5.1, and modified it to take into account the effect of cumuli on aerosols and trace gases in the model. Specifically, the KF-CuP scheme within WRF-Chem represents the impacts of warm cumulus clouds on trace gas and aerosol vertical transport, activation and resuspension of aerosols, aqueous chemistry in clouds, wet removal of aerosol and trace gases, and impacts of aerosol activation on cloud droplet concentrations. Based on simulations in June 2007 in the southern United States, Berg et al. (2015) showed that using KF-CuP could decrease column-integrated BC by up to ~~50~~50 %, due to changes in wet removal, and increase SO_4^{2-} by up to ~~40~~40 % in non-precipitating conditions, due to aqueous chemistry in clouds. However, the long-term or large scale effect of using KF-CuP, or its effect on ozone, has not yet been investigated. These processes are very relevant for the Arctic, where most of the pollution is known to originate from long-range transport (Rahn, 1981; Law et al., 2014), and wet removal is the main process controlling aerosol transport to the Arctic (Mahmood et al., 2016; Raut et al., 2017).

The version of KF-CuP used in this study includes secondary activation of aerosols above the cloud base, which was not included in Berg et al. (2015)~~.~~, and primary activation at cloud base. For primary activation, the model calculates the maximum supersaturation using the Abdul-Razzak and Ghan (2000) parameterization, with the cloud-base updraft speeds from KF-CuP, and the simulated aerosol concentrations in the updrafts. Secondary activation assumes a fixed maximum supersaturation of 0.1 %. Aerosol activation is then calculated from the maximum supersaturations and the critical supersaturations for each aerosol size bin. In addition, KF-CuP is coupled here to the RRTMG radiation scheme, by passing the KF-CuP cloud fraction, cloud water, cloud ice, and cloud droplet numbers to RRTMG, following the approach of Alapaty et al. (2012). The lightning NO_x emissions scheme of Wong et al. (2013), previously coupled in WRF-Chem to other cumulus schemes, is also coupled here with KF-CuP, by linking KF-CuP cloud top heights, cloud fractions, and deep/shallow convection flags to the emission scheme. In this study, we only evaluate the effect of KF-CuP on aerosols and trace gases. These effects are evaluated by disabling in KF-CuP the effect of cumuli on tracer transport, aerosol activitation, aqueous chemistry, and wet removal (NO_KFCUP_CHEM simulation). The effect of lightning NO_x emissions or of the coupling between cumuli and radiation are not evaluated separately here, since they were already studied with other cumulus schemes in Wong et al. (2013) and Alapaty et al. (2012).

3.2 Aerosol sedimentation aloft in the MOSAIC module

In MOSAIC, as it is included in WRF-Chem (and up to the current version 3.8.1 in March 2017), aerosol sedimentation is only implemented in the lowest model level and only takes into account the contribution of sedimentation to dry deposition, but not its role in bringing particles from higher altitudes to the surface. This is discussed but not corrected in Ma et al., 2014. This could be an issue in longer, large-scale simulations, since this could lead to a build-up of large particles (e.g. dust), for which sedimentation is one of the main sinks (Tegen and Fung, 1994). In this study, a first-order explicit sedimentation scheme

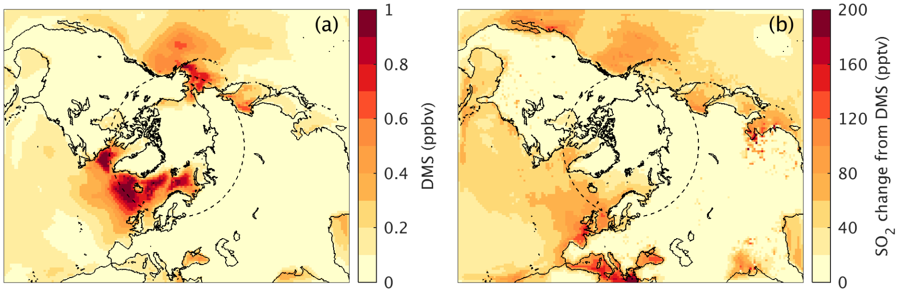

Figure 2. June-July average (a) DMS surface mixing ratios (b) SO_2 surface mixing ratios due to the implementation of DMS emissions and gas-phase chemistry in the model (ALL_UPDATES - NO_DMS).

is implemented above the first vertical level in MOSAIC, using the same algorithm for calculating settling velocities as the one already in use for sedimentation at the model surface. The effects of this change are evaluated by performing a simulation without sedimentation aloft, called NO_SEDIMENTATION; results are discussed in Sect. 4.1.1.

3.3 DMS emissions and gas-phase chemistry for SAPRC-99/MOSAIC

The SAPRC-99/MOSAIC mechanism does not originally include dimethylsulfide (DMS) gas-phase chemistry in WRF-Chem 3.5.1, even though DMS is known to be an important source of SO_2 and sulfate in the Arctic during summer (Li and Barrie, 1993). Here, a simplified representation of SO_2 chemical production from DMS is implemented in SAPRC-99, following the work of Emmons et al. (2010) and Chin et al. (1996). We also use the “online” DMS emission scheme in WRF-Chem, based on Nightingale et al. (2000) and Saltzman et al. (1993), as it was implemented in Marelle et al. (2016). For this study, this scheme is refined by using monthly resolved maps of oceanic DMS from the climatology of Lana et al. (2011) instead of a single oceanic DMS concentration value as in Marelle et al. (2016).

The effects of these updates are evaluated by performing a simulation without DMS chemistry or emissions, called NO_DMS; impacts on aerosols and ozone are discussed in Sect. 4, but we show here in Fig. 2 how this update changes surface DMS and SO_2 in June-July 2008. The modeled amounts and geographical distribution are similar to previous studies (e.g., Boucher et al., 2003). DMS concentrations are especially elevated at higher latitudes due to the high oceanic DMS concentrations. As a result, DMS is also a major source of SO_2, the main precursor for sulfate aerosols (Sect. 4.1.3), over the open Arctic ocean: away from Arctic shipping lanes, DMS emissions and gas-phase chemistry are responsible for 90 to 100 $\%$ of surface SO_2 in this region.

3.4 Coupling dry deposition of trace gases with predicted snow

Dry deposition of trace gases is known to be lower in winter and over snow, due to the reduced stomatal uptake of gases by plants, and due to the enhanced atmospheric stability over snow, i.e. increased surface and aerodynamic resistance to

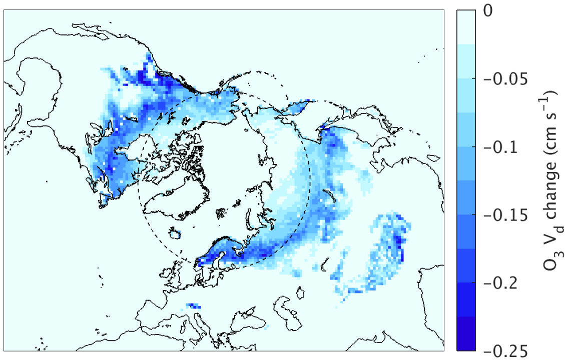

Figure 3. Change in ozone deposition velocity due to the implementation of wintertime dry deposition over seasonal snow (April 2008 average, ALL_UPDATES - NO_SNOWDEP).

deposition. Reduced deposition over seasonal snow cover was already taken into account for the MOZART gas-phase chemistry mechanism in WRF-Chem's deposition scheme (Wesely, 1989), but not for other mechanisms (e.g., SAPRC-99, CBM-Z, RACM). For these other mechanisms, the model only took into account reduced deposition over permanently snow-covered surfaces, e.g. mountain tops, or over sea ice. As a result, Ahmadov et al. (2015) showed that WRF-Chem (run with ~~CBM-Z~~ RACM chemistry) could underestimate observed ozone by more than $5\,\mathrm{ppbv}$ in wintertime conditions in the western United States.

In this study, we also correct WRF-Chem's dry deposition scheme for the SAPRC-99 mechanism, by forcing wintertime conditions in the dry deposition scheme ("Winter, snow on ground and near freezing" seasonal category in WRF-Chem, Wesely, 1989) when predicted snow height is above $10\,\mathrm{cm}$, the threshold already in use in WRF-Chem for the MOZART gas phase chemistry mechanism. Over the snow covered surfaces that were previously treated as vegetation-covered, this update reduces ozone deposition velocities by as much as $-0.25\,\mathrm{cm.s^{-1}}$ during April, as shown in Fig. 3.

3.5 UV-albedo over snow and ice in the Fast-J photolysis scheme

In their study of high wintertime ozone pollution events in the western US, Ahmadov et al. (2015) also identified that the ~~Fast-J photolysis scheme, as~~ photolysis schemes implemented in WRF-Chem 3.5.1 ~~(Barnard et al., 2010) , was~~ were only using one single value for broadband UV albedo at the surface, 0.055, even though this value should be much higher over snow or ice (up to 0.85). In order to correct this, Ahmadov et al. (2015) changed the broadband UV-albedo to 0.85 in their simulations, ~~but this value~~ the value measured at the site of their study. This value cannot be used as such here, since it ~~assumes conditions with 100~~ corresponds to conditions of very high snow cover over bare ground, which are not representative of ~~the~~ our whole simulation region.

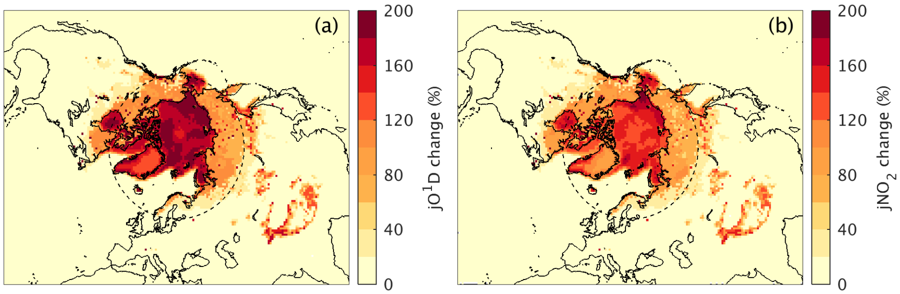

Figure 4. Change in (a) jO^1D and (b) jNO_2 photolysis rates at the surface due to the implementation of an UV-albedo dependence on snow and ice cover in the Fast-J scheme (April 2008 average, ALL_UPDATES - NO_SNOWPHOT).

Here, the UV-albedo in the Fast-J photolysis scheme (Barnard et al., 2010) is calculated as an average (weighted by snow and ice cover) of the snow-free (or ice-free) albedo and the snow-covered (or ice-covered) albedo. This value is updated at each call of the photolysis scheme. Land use-dependent UV-albedo values over snow are taken from the satellite-derived dataset presented in Tanskanen and Manninen (2007), and are retrieved from a look-up table (Table 2 in Tanskanen and Manninen, 2007), based on the WRF-Chem land use category in each grid-cell. The resulting UV-albedo values are much higher than the base value of 0.055, up to 0.85 over $100\ \%$ sea ice or bare snow cover. As a result, photolysis rates predicted by the Fast-J scheme are also greatly increased over snow and ice-covered regions in April, by $+50\ \%$ to $+200\ \%$ for jO^1D and jNO_2 (Fig. 4). The combined effect on surface ozone of this change and of reduced dry deposition over snow are validated and discussed in Sect. 4.2.1 and 4.2.2.

3.6 Heat sink from melting sea ice in the Noah land surface model

In WRF version 3.5.1, the Noah Land Surface Model did not take into account the heat sink due to sea ice melt (latent heat of ice melt) in the energy budgets at the prescribed sea ice surface. As a result, the surface model could predict unrealistically high surface temperatures during the ice melt season. We corrected this issue by simply prescribing the skin temperature of sea ice to $0\ \mathrm{K}$ when the model diagnoses surface melt. We have shared this update with the WRF community, and it was included in WRF-Chem after version 3.7.1. Implementing this correction can decrease 2-meter temperatures over sea ice by as much as $10\ \mathrm{K}$ during the melt season. This is of concern since the temperature contrast between snow and sea-ice covered and snow and sea-ice free areas is one of the main factors determining the location of the Arctic dome (Stohl, 2006; Klonecki et al., 2003), whose northward retreat during summer isolates the Arctic surface from pollution transported from the midlatitudes. As a result, erroneously small latitudinal temperature contrasts could greatly increase long-range pollution transport to the Arctic surface during summer. However, the exact magnitude of this effect on Arctic aerosols and ozone has not been evaluated until now (this is discussed and validated in Sect. 4).

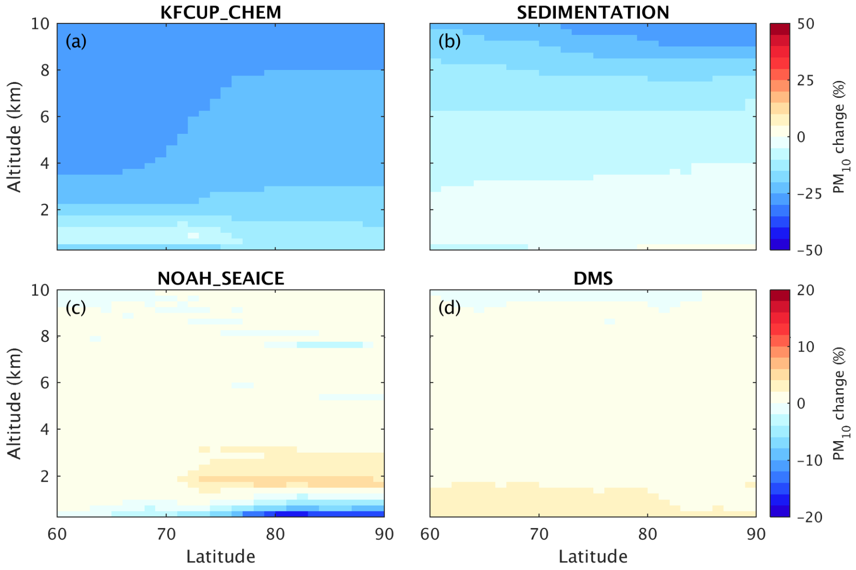

Figure 5. Change in the April-July 2008 average zonal mean PM_{10} due to (a) KF-CuP cumulus effect on aerosols and trace gases, (b) aerosol sedimentation aloft, (c) the sea ice melt heat sink in Noah-LSM and (d) DMS emissions and chemistry. Note the differences in scale between top and bottom panels.

4 Effect of the model updates on aerosol and ozone concentrations in the Arctic.

This section presents the effect of individual model updates on modeled aerosols (Sect. 4.1.1) and ozone (Sect. 4.2.1) in the Arctic. The new, updated version of the model is also validated against airborne (Sect. 4.1.2) and surface (Sect. 4.1.3 and 4.2.2) measurements of aerosols and ozone in the Arctic in 2008. Simulation performance is evaluated in terms of root mean square error (RMSE), defined as

$$\frac{1}{n}\sqrt{\sum_{i=1}^{n}(x_{mod,i}-x_{obs,i})^2} \qquad (1)$$

where x_{mod} and x_{obs} are respectively the modeled and observed mass concentrations or volume mixing ratios.

4.1 Aerosols

4.1.1 Effect on zonal mean aerosol concentrations in the Arctic

The effect of the KFCUP_CHEM, SEDIMENTATION, NOAH_SEAICE and DMS updates on zonal mean total aerosol mass concentrations (which are equivalent to zonal mean PM_{10} in WRF-Chem/MOSAIC) are presented in Fig. 5. The effect of the updated trace gas deposition and photolysis over snow and ice (SNOWDEP, SNOWPHOT) on PM_{10} (not shown) is very low,

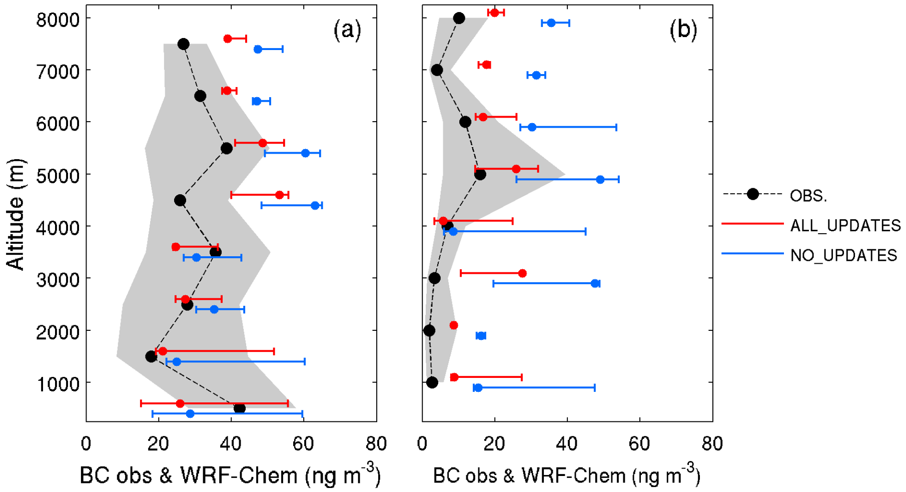

Figure 6. ARCTAS (a) spring and (b) summer median SP2 rBC (size range 90 nm–1000 nm) profiles north of latitude 70°N (black, gray shading indicates 25th and 75th percentile), and WRF-Chem median BC (size range 80 nm–1000 nm) profiles interpolated along the same ARCTAS flights (red, ALL_UPDATES; blue, NO_UPDATES, error bars indicate 25th and 75th percentile).

less than 1 $\%$. Fig. 5 shows that aerosol sedimentation aloft (SEDIMENTATION) and cumulus effects on aerosols and trace gases (KFCUP_CHEM) have the largest impact on aerosols in the Arctic, -30 $\%$ at higher altitudes. Sedimentation aloft is both a sink (particles transported below) and a source (particles transported from above) of particles at lower altitudes, which explains why it has little effect below 3 km. The net effect of KF-CuP is to decrease aerosol mass; this indicates that the effect is dominated by increased wet removal, as in Berg et al. (2015), and is not compensated by increased sulfate formation in the aqueous phase (cloud chemistry) or by increased vertical aerosol precursor and aerosol transport (tracer convection).

The implementation of the sea ice melt heat sink in Noah-LSM strongly reduces PM_{10} at the Arctic surface (< -20 $\%$), and increases aerosol concentrations aloft. In these simulations, local sources of pollution at the sea ice surface are negligible; because of this, aerosol concentrations there are mostly due to downward mixing of aerosols and gases from the free troposphere. The NOAH_SEAICE updates reduces surface temperatures over sea ice during summer, increasing stability, decreasing vertical mixing, thus reducing this tropospheric source (sink) of surface (free troposphere) pollution. DMS emissions and chemistry increase PM_{10} by $+2$ to $+4$ $\%$, due to increased SO_4^{2-} aerosols formed from SO_2 in the marine boundary layer. However, relative increases of PM_{10} from DMS remain rather low because of the relative lack of open water for DMS emissions north of 60° N, and the high background PM_{10} in these areas due to co-located emissions of sea salt aerosols.

4.1.2 Validation against BC profiles from the ARCTAS aircraft campaign

In order to validate the modeled aerosol distribution, we compare in Fig. 6 results from the ALL_UPDATES and NO_UPDATES simulations to vertical profiles of refractory BC (rBC) measured by SP2 (single particle soot photometer) during the ARCTAS

Table 3. RMSE of individual WRF-Chem simulations relative to Arctic observations of aerosols and ozone. All sensitivity simulations are performed by deactivating updates from the ALL_UPDATES simulation; as a result, any increase in RMSE relative to ALL_UPDATES indicates that a given update improved RMSE. For surface measurements, RMSEs are calculated at each station and given as a network average.

Simulation name	ARCTAS spring BC (ng.m^{-3})	ARCTAS summer BC (ng.m^{-3})	Surface BC (ng.m^{-3})	Surface SO$_4$ (ng.m^{-3})	Surface O$_3$ (ppbv)
ALL_UPDATES	**13.5**	**11.6**	**14.2**	**261**	**7.56**
NO_UPDATES	18.8	25.4	23.0	332	8.89
NO_SEDIMENTATION	13.6	11.7	14.5	270	7.56
NO_KFCUP_CHEM	18.7	24.2	17.6	285	7.97
NO_NOAH_SEAICE	13.4	11.6	16.8	309	7.54
NO_DMS	13.5	11.3	14.4	263	7.61
NO_SNOWDEP_SNOWPHOT	13.5	11.6	14.4	279	8.35
AMAP (2015) and Eckhardt et al. (2015)	13.8	38.8	34.8	493	9.4

(Arctic Research of the Composition of the Troposphere from Aircraft and Satellites) campaigns in April and July 2008 (Jacob et al., 2010; Matsui et al., 2011). As in Eckhardt et al. (2015), this comparison only includes observations and model results north of latitude 70° N. The updated model is in much better agreement with observations than the original NO_UPDATES simulation, especially in the summer, where RMSE decreases by $13.8\ \mathrm{ng.m^{-3}}$ in ALL_UPDATES. Table 3 shows that the decreased model error is almost solely due $(-12.6\ \mathrm{ng.m^{-3}})$ to the KFCUP_CHEM update. Other updates have little effect, which is understandable since small BC-containing particles have slow sedimentation velocities, are not directly affected by DMS, and because the NOAH_SEAICE update has the largest effect at the sea-ice surface, which was not sampled by the aircraft. The ~~updated~~ updates have little effect on correlation coefficients, which rise from 0.07 to 0.08 in spring, and decrease from 0.48 to 0.43 during summer, indicating that neither the base model nor the updated version are able to reproduce well the vertical variability of BC in the Arctic troposphere. In addition, the updated model still overestimates observations in summer, which could be due to overestimated emissions from e.g. biomass burning, or underestimated removal. Raut et al. (2017) showed that increasing the horizontal resolution from $100\ \mathrm{km}$ to $40\ \mathrm{km}$ could reduce summertime BC simulated by WRF-Chem by 25–30 %, by improving the representation of wet removal.

4.1.3 Validation against surface measurements of BC and SO$_4^{2-}$ in the Arctic

WRF-Chem simulation results are evaluated in Fig. 7 against surface equivalent BC (eBC) and non-sea-salt sulfate measurements in the Arctic. eBC is calculated based on light absorption measurements by Particle Soot Absorption Photometers (PSAP), and converted to concentrations by assuming a value for mass-absorption efficiency. As a result, the uncertainty in eBC measurement is of at least a factor of 2 (Bond et al., 2013). SO$_4^{2-}$ is obtained from filters and analyzed by ion chromatography. The contribution from sea salt is removed to obtain a non-seasalt sulfate concentration comparable with WRF-Chem aerosol sulfate. Additional details about these measurements are given in Eckhardt et al. (2015).

In terms of BC, the updated model run (ALL_UPDATES) agrees much better with surface eBC measurements than the NO_UPDATES simulation, especially during summer (decreasing RMSE by $-8.8\ \mathrm{ng.m^{-3}}$). ~~The seasonal cycle of BC pollution is also improved.~~ Table 3 shows that this is mostly due to the implementation of the KFCUP_CHEM ($-3.4\ \mathrm{ng.m^{-3}}$ of RMSE) and NOAH_SEAICE ($-2.6\ \mathrm{ng.m^{-3}}$ of RMSE) updates, other updates having very litle effect ($< 0.3\ \mathrm{ng.m^{-3}}$ change in RMSE). The average Pearson correlation coefficient increases from 0.43 to 0.87, indicating that the seasonal cycle of BC pollution is also improved in the model.

For sulfate, the updated model performs much better at Alert and Barrow during summer, and slightly better at other stations, due to the competing effects of increased sulfate from DMS and decreased sulfate from KFCUP_CHEM and NOAH_SEAICE. Surprisingly, DMS has relatively little effect on the $\mathrm{SO_4^{2-}}$ RMSE on average (Table 3). This is because including DMS emissions and gas-phase chemistry improves RMSE at Pallas (Finland), Alert (Canada), Nord (Greenland) and Barrow (Alaska) (-11 to $-27\ \mathrm{ng.m^{-3}}$) but degrades RMSE at Zeppelin (Svalbard) ($+66\ \mathrm{ng.m^{-3}}$), where the model already overestimates sulfate. Another surprising result is the impact of dry deposition and UV-albedo updates on sulfate (Table 3). This effect is likely mediated by changes in oxidants (OH and ozone, as discussed in Sect. 4.2.1) and their impacts on $\mathrm{SO_2}$ oxidation. These updates also improve the modeled seasonal cycle of sulfate, increasing the average Pearson correlation coefficient from 0.28 to 0.73. Both NO_UPDATES and ALL_UPDATES tend to be biased low in April (especially at the most remote Arctic sites, Alert, Barrow and Nord), which could be due to underestimated long-range transport caused by the limited resolution (Sato et al., 2016).

4.2 Ozone

4.2.1 Effect on surface ozone in the Arctic

The effect of the SNOWDEP_SNOWPHOT, NOAH_SEAICE, KFCUP_CHEM and DMS updates on surface $\mathrm{O_3}$ concentrations in the Arctic is shown in Fig. 8. The effect of aerosol sedimentation aloft (SEDIMENTATION) on ozone is very low and is not shown. The updates related to deposition and photolysis over frozen surfaces have a strong effect on surface $\mathrm{O_3}$. Based on the 1-month long simulations NO_SNOWDEP and NO_SNOWPHOT in April, we find that this is mostly due to changes in dry deposition ($+10$ ppbv in April, against $+1$ to $+2$ ppbv for photolysis). Ozone also decreases slightly over sea-ice with the SNOWDEP_SNOWPHOT update. This is likely due to the UV flux increase from the SNOWPHOT update, since ozone formation in the Arctic boundary layer is $\mathrm{NO_x}$-limited (Jacob et al., 1992), and ozone increases when the UV-flux decreases in $\mathrm{NO_x}$-limited regions (Liu and Trainer, 1988). Ozone concentrations at the surface are strongly reduced by the NOAH_SEAICE update (down to -10 ppbv), due to the increased stability and lower influx of ozone precursors and ozone from the free troposphere to the surface. The KFCUP_CHEM update also has a strong effect on ozone ($+2$ to $+5$ ppbv), especially at lower latitudes where convection occurs. This could be due to tracer transport by mid-level convective clouds, bringing polluted air down to the surface (Lelieveld and Crutzen, 1994). Adding DMS leads to a modest decrease in surface

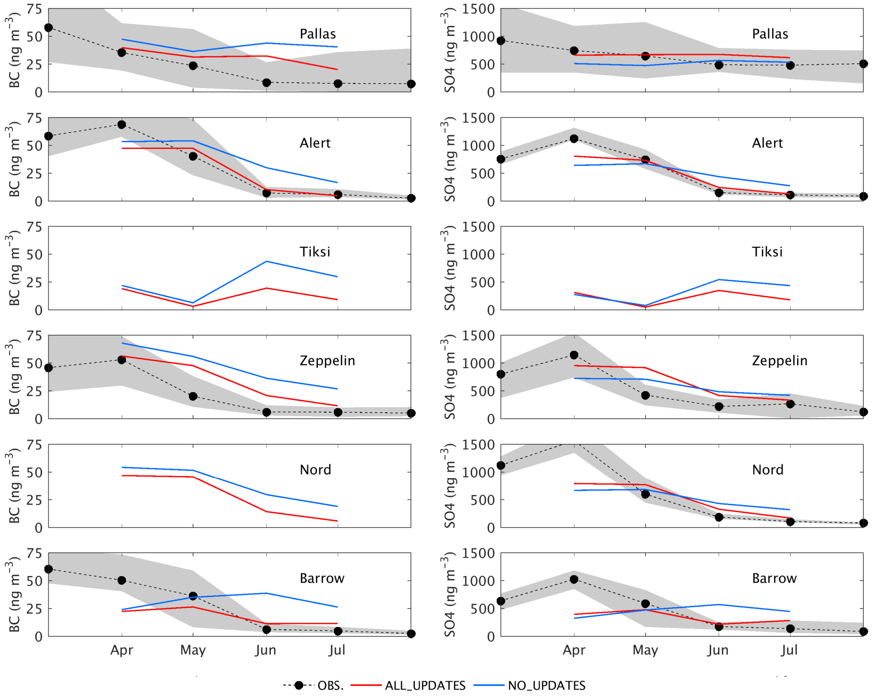

Figure 7. Monthly median BC (left) and SO_4^{2-} (right) observations at Arctic surface stations (black, gray shading indicates 25th and 75th percentile), and corresponding WRF-Chem results (red, ALL_UPDATES; blue, NO_UPDATES).

ozone over the open ocean (-2 ppbv at most), which is associated with a decrease in NO_x mixing ratios (-10 to -20 %), due to an increased HNO_3 sink ($+5$ to $+20$ %) from increased N_2O_5 uptake on the additional sulfate aerosols (-20 to -90 % N_2O_5 at the sea surface).

4.2.2 Validation against surface measurements of ozone in the midlatitudes and in the Arctic

WRF-Chem results from the ALL_UPDATES and NO_UPDATES simulations are evaluated against surface ozone measurements from the EMEP (European Monitoring and Evaluation Programme) European network and the CASTNET (Clean Air Status and Trends Network) US network, in addition to ozone measurements from the Barrow (Alaska) and Summit (Greenland) polar observatories of NOAA-ESRL (National Oceanic and Atmospheric Administration, Earth System Research Laboratory). The evaluation against Arctic stations (north of 60° N, $17/228$ stations) is shown in Fig. 9b. When all updates are included, RMSE is reduced for all seasons (-1.3 ppbv on average), even though the ALL_UPDATES simulations sometimes overestimate ozone in spring. This overestimation is clearly due to the fact that WRF-Chem has no treatment of halogen chemistry in the model, which is responsible for ozone depletion events in polar regions during spring (e.g., Simpson et al., 2007; Abbatt et al., 2012). Table 3 shows that improvements in RMSE are mostly due to the SNOWDEP_SNOWPHOT update (-0.8 ppbv RMSE), and to the KFCUP_CHEM update (-0.4 ppbv RMSE). The average Pearson correlation coefficient

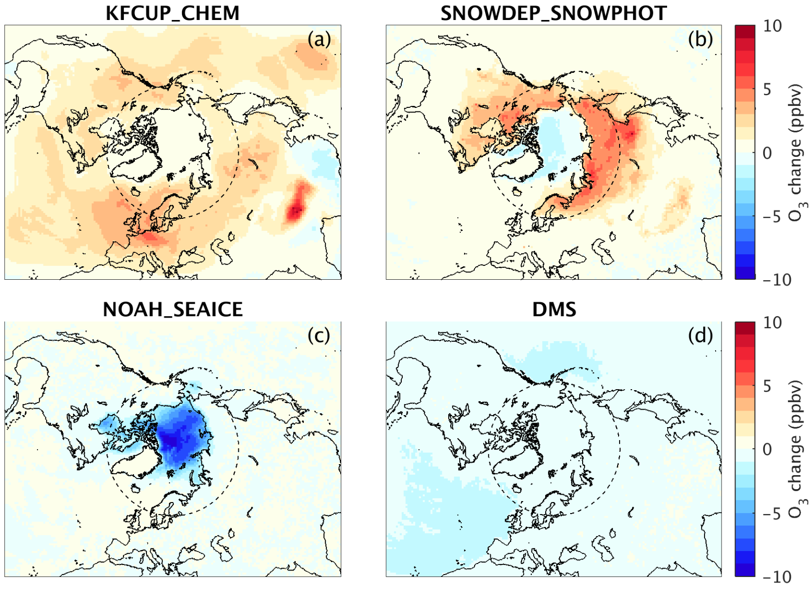

Figure 8. Change in the April to July average surface ozone due to (a) KF-CuP cumulus effect on aerosol and trace gases, (b) improved trace gas deposition over snow and improved UV-albedo for photolysis over snow and ice, (c) sea ice melt heat sink in Noah-LSM and (d) DMS emissions and gas-phase chemistry. .

also increases from 0.67 to 0.73 in the updated model, only due to the SNOWDEP_SNOWPHOT update. The effect of the NOAH_SEAICE update is low, since only stations Nord in Northern Greenland and Barrow in Alaska are located in an area with significant summer sea ice where this change affecting surface mixing ratios could play a role. Figure 9 shows that these updates also have a relatively strong effect over the whole measurement network, including subarctic sites, indicating that these processes should also be taken into account when studying ozone at lower latitudes with WRF-Chem. At subarctic sites (south of 60° N), model updates decrease RMSE by 13 % on average, and by more than 50 % at 9 surface sites. These improvements in the midlatitudes are mostly due to the KFCUP SUBSCRIPTNBCHEM update, and to the SNOWDEP SUBSCRIPTNBSNOWPHOT update at sites where seasonal snow is present. Ahmadov et al. (2015) , using WRF-Chem 3.5.1, also showed that reduced deposition and enhanced photolysis over snow could contribute to high wintertime ozone in the United States, when other favorable conditions were present, such as shallow boundary layers and high emissions.

4.3 Discussion about the differences with the quasi-hemispheric WRF-Chem simulation in Eckhardt et al. (2015) and AMAP (2015)

The ALL_UPDATES simulation performs better than the WRF-Chem 3.5.1 simulation presented in Eckhardt et al. (2015) and AMAP (2015). Compared to these earlier results, RMSE is improved in ALL_UPDATES by $0.3\ \mathrm{ng.m^{-3}}$ for ARCTAS Spring

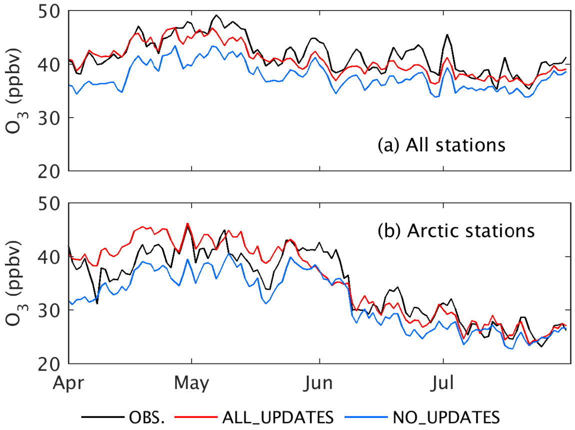

Figure 9. Comparison between daily averaged surface ozone measurements (black) and WRF-Chem results (red, ALL_UPDATES; blue, NO_UPDATES) (a) averaged over all stations within the domain (228 stations) (b) averaged over Arctic stations only (latitude $>$ 60° N, $17/228$ stations).

rBC, by $27.2\ \mathrm{ng.m^{-3}}$ for ARCTAS summer rBC, by $20.6\ \mathrm{ng.m^{-3}}$ for surface BC, by $232\ \mathrm{ng.m^{-3}}$ for surface $\mathrm{SO_4^{2-}}$ and by $1.84\ \mathrm{ppbv}$ for surface ozone (Table 3). However, the NO_UPDATES simulations also performs better than the simulation in Eckhardt et al. (2015) and AMAP (2015), compared to most datasets (respectively, RMSE higher by $5.0\ \mathrm{ng.m^{-3}}$, lower by $13.4\ \mathrm{ng.m^{-3}}$, lower by $11.8\ \mathrm{ng.m^{-3}}$, lower by $161\ \mathrm{ng.m^{-3}}$ and lower by $0.51\ \mathrm{ppbv}$). This indicates that the model updates presented here are only partly responsible for this improved RMSE, and that differences in setup between the simulations also play a large role.

There are many differences in model setup between the simulation in Eckhardt et al. (2015) and AMAP (2015) and the ones presented here. The most significant are (1) the change of the gas-phase chemistry scheme (SAPRC-99 here and CBM-Z earlier, but both being coupled to MOSAIC-8 bin aerosols including aqueous chemistry), (2) the different fire emission inventories (daily FINNv1.5 emissions here, monthly GFEDv3.1, Global Fire Emissions Database, emissions earlier), (3) the larger simulation domain used here, extending down to latitudes 10–35° N (Fig. 1), instead of 28–45° N earlier (4) the inclusion of lightning $\mathrm{NO_x}$ emissions here. Although it is difficult to attribute precisely the improvement to each of these changes, the change in fire emissions likely had a strong effect on modeled BC, since we find that GFEDv3.1 BC emissions north of 60° N used in earlier WRF-Chem simulations were 1.5 and 3.9 times higher in June and July than FINNv1.5 BC emissions used here, a point also discussed in AMAP (2015). Another likely driver of errors for aerosols is the relatively small simulation domain used earlier. This could have made WRF-Chem results too dependent on the lateral boundary conditions from the MOZART-4 global model, in which aerosols are represented by a simpler bulk aerosol scheme. The change of gas phase mechanism, the use of a lightning $\mathrm{NO_x}$ emissions scheme and the larger simulation domain used here also likely had an impact on ozone results in the Arctic.

5 Conclusions

In this study, we update the WRF-Chem ~~model and~~ 3.5.1 model (with SAPRC-99 gas-phase chemistry and MOSAIC aerosols) and perform quasi-hemispheric simulations of aerosols and ozone in the Arctic region. This allows us to draw the following main conclusions and perspectives:

(1) *Improved aerosols and ozone simulated by WRF-Chem 3.5.1 in the Arctic.* ~~Errors for~~ Updating the model greatly reduces model errors compared to previous WRF-Chem evaluations in the Arctic (e.g., Eckhardt et al., 2015) . Specific simulations with and without each model update allows us to characterize which process has the most effect on Arctic pollution distributions. Simulated airborne and surface BC in the Arctic are ~~greatly reduced compared to previous results (Eckhardt et al., 2015) by including the KF-CuP scheme that treats cumulus effects~~ particularly sensitive to the effect of cumulus clouds on aerosols and trace gases (~~including~~ wet removal, aerosol activation, tracer transport and cloud chemistry, represented by the KF-CuP scheme), and by ~~correcting modeled~~ the representation of skin temperatures over sea-ice, affecting stability, in the Noah land surface ~~modules. Adding these processes~~model. Implementing these two updates, as well as DMS ~~emissions and~~ gas-phase chemistry, also improves the representation of sulfate concentrations in the Arctic, although ~~increases in sulfate from~~ the simple DMS chemistry scheme ~~included here could be too high~~ used here appears to overestimate sulfate production at one Arctic site (Zeppelin). ~~Neglecting~~ In our simulations, neglecting sedimentation aloft does not have a significant impact on BC or sulfate concentrations, and has relatively little influence on total aerosol concentrations~~in our simulations~~, except in the upper troposphere. ~~The implementation of KF-Cup chemistry and the corrections to~~ Model updates also improve simulated ozone, both in the Arctic and in the midlatitudes. The corrections to skin temperatures in Noah-LSM ~~also~~ have a strong impact on ozone ~~in the Arctic (+2~~ over sea ice (-5 to ~~$+5$~~-10 ppbv~~for KF-CuP~~), ~~-5~~ while the implementation of KF-CuP increases ozone by $+2$ to ~~-10~~$+5$ ppbv ~~over sea ice for Noah-LSM), but the~~ both in the Arctic and at lower latitudes. The main source of improvement over land appears to be the implementation of a snow and ice-dependent UV-albedo for the Fast-J photolysis scheme, and the decrease of deposition velocities over snow-covered ground ($> +10$ ppbv combined effect in spring where seasonal snow is present, in the Arctic and in the midlatitudes). However, implementing these processes can sometimes degrade model performance in the Arctic spring, by increasing ozone levels ~~that are sometimes~~ already overestimated because of the lack of halogen chemistry ~~that depletes ozone at the surface~~in the gas-phase mechanism.

(2) *Identification of potential areas of further improvement in the WRF-Chem model.* The main discrepancies between modeled and observed ozone in the Arctic occur in spring at coastal Arctic sites (e.g. Barrow, Alert, Nord), where ozone depletion by halogen chemistry occurs. ~~As a result, in~~ In order to study springtime Arctic ozone it seems critical to include these processes in WRF-Chem, as discussed earlier, in e.g. ~~in~~ AMAP (2015). WRF-Chem underestimates surface aerosol surface concentrations in spring, which could be due to underestimation of long-range transport due to the limited horizontal resolution. Ma et al. (2013) found little improvement in BC transport when decreasing the resolution from 2° to 1°, but recent research (Sato et al., 2016) indicates that BC transport to the Arctic could be ~~significantly higher for~~ enhanced in WRF-Chem simulations at much finer resolutions (< 10 km). ~~In addition, the updated WRF-Chem model still overestimates BC concentrations aloft during summer , although this bias is greatly reduced~~ Simulations with the updated model have significantly lower RMSE for

airborne BC during summer (−54 %~~of RMSE)by the developments presented here~~), but the model still overestimates BC aloft significantly in this season. This could also be due to the low resolution, or to underestimated removal processes (Raut et al., 2017), since the model does not currently represent aerosol activation in ice clouds, and only includes a simplified treatment of secondary activation in deep convective clouds. Emissions from boreal fires could also be an important source of uncertainty during summer, and for this reason it is important to validate the different fire emission inventories in the Arctic.

(3) *Definition of a model setup that can be used in future work to study aerosol and ozone pollution at continental scales in the Arctic.* The updated model setup presented in this paper improves simulation of BC, sulfate and ozone in the Arctic. The updated results now appear to be in better agreement than most global models included in the recent intercomparisons of Eckhardt et al. (2015) and AMAP (2015), although further model intercomparisons are needed to confirm this. There are many pressing issues concerning short-lived pollutants in the Arctic and their climate impacts which require reliable model results at the hemispheric scale. For example, the relative importance of the different pollution sources to Arctic pollution is still uncertain (local vs. remote, fossil fuel vs. biomass burning, natural vs. anthropogenic). In addition, the attribution of recent trends in Arctic composition can be difficult if long-range transport from different source regions is not correctly reproduced. Other Arctic issues could also benefit from accurate large-scale regional simulations, such as the impact of Arctic air pollution on ecosystems (i.e. through deposition) and a more precise quantification of the climate impacts of cloud-aerosol interactions in the Arctic and of BC deposition on snow (Arnold et al., 2016).

6 Code availability

The WRF-Chem code is available at http://www2.mmm.ucar.edu/wrf/users/download/get_source.html. After version 3.8, it includes the KF-CuP scheme and, after version 3.7.1, the sea ice correction in the Noah-LSM module presented in this paper. Other updates will be proposed for implementation in the next WRF-Chem version, or can be obtained from Louis Marelle (louis.marelle@cicero.oslo.no) upon request.

Author contributions. The first author (LM) developped and implemented the updates, performed the simulations and the analysis and drafted the paper. JCR, KSL and JLT contributed to simulation design, to the interpretation of results, and to writing the manuscript. The WRF-Chem 3.5.1 code with latest KF-CuP and SOA developments was provided by PNNL authors (JDF, LKB, RCE, MS), who also advised on how to perform futher coupling between WRF-Chem and the KF-Cup code (LKB, RCE) and how to simplify the SOA scheme (MS). All co-authors contributed to the manuscript and to the analysis.

Acknowledgements. L. Marelle acknowledges funding from TOTAL SA through an ANRT CIFRE PhD grant. We also acknowledge support from the French Pollution in the Arctic System (PARCS) project funded as part of the French Arctic Initiative by CNRS. We thank Sabine Eckhardt and Marianne T. Lund for providing us the surface measurements of black carbon and sulfate in the Arctic. Computing resources were provided by IDRIS HPC resources (GENCI allocations 2015-017141 and 2016-017141) and the IPSL mesoscale computing center (CICLAD: Calcul Intensif pour le Climat, l’Atmosphère et la Dynamique). J.D. Fast, L.K. Berg, R.C. Easter, and M. Shrivastava were supported by the Office of Science of the U.S. Department of Energy as part of the Atmospheric System Research (ASR) program. The Pacific Northwest National Laboratory (PNNL) is operated by DOE by the Battelle Memorial Institute under contract DE-A06-76RLO976 1830.

References

Abbatt, J. P. D., Thomas, J. L., Abrahamsson, K., Boxe, C., Granfors, A., Jones, A. E., King, M. D., Saiz-Lopez, A., Shepson, P. B., Sodeau, J., Toohey, D. W., Toubin, C., von Glasow, R., Wren, S. N., and Yang, X.: Halogen activation via interactions with environmental ice and snow in the polar lower troposphere and other regions, Atmospheric Chemistry and Physics, 12, 6237–6271, doi:10.5194/acp-12-6237-2012, http://www.atmos-chem-phys.net/12/6237/2012/, 2012.

Abdul-Razzak, H. and Ghan, S. J.: A parameterization of aerosol activation: 2. Multiple aerosol types, Journal of Geophysical Research: Atmospheres, 105, 6837–6844, doi:10.1029/1999JD901161, http://dx.doi.org/10.1029/1999JD901161, 2000.

Ahmadov, R., McKeen, S., Trainer, M., Banta, R., Brewer, A., Brown, S., Edwards, P. M., de Gouw, J. A., Frost, G. J., Gilman, J., Helmig, D., Johnson, B., Karion, A., Koss, A., Langford, A., Lerner, B., Olson, J., Oltmans, S., Peischl, J., Pétron, G., Pichugina, Y., Roberts, J. M., Ryerson, T., Schnell, R., Senff, C., Sweeney, C., Thompson, C., Veres, P. R., Warneke, C., Wild, R., Williams, E. J., Yuan, B., and Zamora, R.: Understanding high wintertime ozone pollution events in an oil- and natural gas-producing region of the western US, Atmospheric Chemistry and Physics, 15, 411–429, doi:10.5194/acp-15-411-2015, http://www.atmos-chem-phys.net/15/411/2015/, 2015.

Alapaty, K., Herwehe, J. A., Otte, T. L., Nolte, C. G., Bullock, O. R., Mallard, M. S., Kain, J. S., and Dudhia, J.: Introducing subgrid-scale cloud feedbacks to radiation for regional meteorological and climate modeling, Geophysical Research Letters, 39, doi:10.1029/2012GL054031, http://dx.doi.org/10.1029/2012GL054031, l24809, 2012.

AMAP: AMAP Assessment 2015: Black carbon and ozone as Arctic climate forcers, Tech. rep., Arctic Monitoring and Assessment Programme (AMAP), Oslo, Norway, 2015.

Arnold, S., Law, K., Brock, C., Thomas, J., Starkweather, S., von Salzen, K., Stohl, A., Sharma, S., Lund, M., Flanner, M., Petäjä, T., Tanimoto, H., Gamble, J., Dibb, J., Melamed, M., Johnson, N., Fidel, M., Tynkkynen, V.-P., Baklanov, A., Eckhardt, S., Monks, S., Browse, J., and Bozem, H.: Arctic air pollution: Challenges and opportunities for the next decade, Elementa, 4, 104, doi:http://doi.org/10.12952/journal.elementa.000104, 2016.

Arnold, S. R., Emmons, L. K., Monks, S. A., Law, K. S., Ridley, D. A., Turquety, S., Tilmes, S., Thomas, J. L., Bouarar, I., Flemming, J., Huijnen, V., Mao, J., Duncan, B. N., Steenrod, S., Yoshida, Y., Langner, J., and Long, Y.: Biomass burning influence on high-latitude tropospheric ozone and reactive nitrogen in summer 2008: a multi-model analysis based on POLMIP simulations, Atmospheric Chemistry and Physics, 15, 6047–6068, doi:10.5194/acp-15-6047-2015, http://www.atmos-chem-phys.net/15/6047/2015/, 2015.

Barnard, J. C., Fast, J. D., Paredes-Miranda, G., Arnott, W. P., and Laskin, A.: Technical Note: Evaluation of the WRF-Chem "Aerosol Chemical to Aerosol Optical Properties" Module using data from the MILAGRO campaign, Atmospheric Chemistry and Physics, 10, 7325–7340, doi:10.5194/acp-10-7325-2010, http://www.atmos-chem-phys.net/10/7325/2010/, 2010.

Berg, L. K. and Stull, R. B.: A Simple Parameterization Coupling the Convective Daytime Boundary Layer and Fair-Weather Cumuli, Journal of the Atmospheric Sciences, 62, 1976–1988, doi:10.1175/JAS3437.1, http://dx.doi.org/10.1175/JAS3437.1, 2005.

Berg, L. K., Jr., W. I. G., Kassianov, E. I., and Deng, L.: Evaluation of a Modified Scheme for Shallow Convection: Implementation of CuP and Case Studies, Monthly Weather Review, 141, 134–147, doi:10.1175/MWR-D-12-00136.1, http://dx.doi.org/10.1175/MWR-D-12-00136.1, 2013.

Berg, L. K., Shrivastava, M., Easter, R. C., Fast, J. D., Chapman, E. G., Liu, Y., and Ferrare, R. A.: A new WRF-Chem treatment for studying regional-scale impacts of cloud processes on aerosol and trace gases in parameterized cumuli, Geoscientific Model Development, 8, 409–429, doi:10.5194/gmd-8-409-2015, http://www.geosci-model-dev.net/8/409/2015/, 2015.

Bond, T. C., Doherty, S. J., Fahey, D. W., Forster, P. M., Berntsen, T., DeAngelo, B. J., Flanner, M. G., Ghan, S., Kärcher, B., Koch, D., Kinne, S., Kondo, Y., Quinn, P. K., Sarofim, M. C., Schultz, M. G., Schulz, M., Venkataraman, C., Zhang, H., Zhang, S., Bellouin, N., Guttikunda, S. K., Hopke, P. K., Jacobson, M. Z., Kaiser, J. W., Klimont, Z., Lohmann, U., Schwarz, J. P., Shindell, D., Storelvmo, T., Warren, S. G., and Zender, C. S.: Bounding the role of black carbon in the climate system: A scientific assessment, Journal of Geophysical Research: Atmospheres, 118, 5380–5552, doi:10.1002/jgrd.50171, http://dx.doi.org/10.1002/jgrd.50171, 2013.

Boucher, O., Moulin, C., Belviso, S., Aumont, O., Bopp, L., Cosme, E., von Kuhlmann, R., Lawrence, M. G., Pham, M., Reddy, M. S., Sciare, J., and Venkataraman, C.: DMS atmospheric concentrations and sulphate aerosol indirect radiative forcing: a sensitivity study to the DMS source representation and oxidation, Atmospheric Chemistry and Physics, 3, 49–65, doi:10.5194/acp-3-49-2003, http://www.atmos-chem-phys.net/3/49/2003/, 2003.

Browse, J., Carslaw, K. S., Arnold, S. R., Pringle, K., and Boucher, O.: The scavenging processes controlling the seasonal cycle in Arctic sulphate and black carbon aerosol, Atmospheric Chemistry and Physics, 12, 6775–6798, doi:10.5194/acp-12-6775-2012, http://www.atmos-chem-phys.net/12/6775/2012/, 2012.

Carter, W. P. L.: Documentation of the SAPRC-99 chemical mechanism for VOC reactivity assessment. Final Report to California Air Resources Board Contract 92-329 and Contract 95-308,, Tech. rep., Air Pollution Research Center and College of Engineering Center for Environmental Research and Technology, University of California Riverside, California, 2000.

Chen, F. and Dudhia, J.: Coupling an Advanced Land Surface-Hydrology Model with the Penn State-NCAR MM5 Modeling System. Part I: Model Implementation and Sensitivity, Mon. Wea. Rev., 129, 569–585, doi:10.1175/1520-0493(2001)129<0569:CAALSH>2.0.CO;2, http://dx.doi.org/10.1175/1520-0493(2001)129<0569:CAALSH>2.0.CO;2, 2001.

Chin, M., Jacob, D. J., Gardner, G. M., Foreman-Fowler, M. S., Spiro, P. A., and Savoie, D. L.: A global three-dimensional model of tropospheric sulfate, Journal of Geophysical Research: Atmospheres, 101, 18 667–18 690, doi:10.1029/96JD01221, http://dx.doi.org/10.1029/96JD01221, 1996.

Chin, M., Ginoux, P., Kinne, S., Torres, O., Holben, B. N., Duncan, B. N., Martin, R. V., Logan, J. A., Higurashi, A., and Nakajima, T.: Tropospheric Aerosol Optical Thickness from the GOCART Model and Comparisons with Satellite and Sun Photometer Measurements, J. Atmos. Sci., 59, 461–483, doi:10.1175/1520-0469(2002)059<0461:TAOTFT>2.0.CO;2, http://dx.doi.org/10.1175/1520-0469(2002)059<0461:TAOTFT>2.0.CO;2, 2002.

Eckhardt, S., Quennehen, B., Olivié, D. J. L., Berntsen, T. K., Cherian, R., Christensen, J. H., Collins, W., Crepinsek, S., Daskalakis, N., Flanner, M., Herber, A., Heyes, C., Hodnebrog, Ø., Huang, L., Kanakidou, M., Klimont, Z., Langner, J., Law, K. S., Lund, M. T., Mahmood, R., Massling, A., Myriokefalitakis, S., Nielsen, I. E., Nøjgaard, J. K., Quaas, J., Quinn, P. K., Raut, J.-C., Rumbold, S. T., Schulz, M., Sharma, S., Skeie, R. B., Skov, H., Uttal, T., von Salzen, K., and Stohl, A.: Current model capabilities for simulating black carbon and sulfate concentrations in the Arctic atmosphere: a multi-model evaluation using a comprehensive measurement data set, Atmospheric Chemistry and Physics, 15, 9413–9433, doi:10.5194/acp-15-9413-2015, http://www.atmos-chem-phys.net/15/9413/2015/, 2015.

Emmons, L. K., Walters, S., Hess, P. G., Lamarque, J.-F., Pfister, G. G., Fillmore, D., Granier, C., Guenther, A., Kinnison, D., Laepple, T., Orlando, J., Tie, X., Tyndall, G., Wiedinmyer, C., Baughcum, S. L., and Kloster, S.: Description and evaluation of the Model for Ozone and Related chemical Tracers, version 4 (MOZART-4), Geoscientific Model Development, 3, 43–67, doi:10.5194/gmd-3-43-2010, http://www.geosci-model-dev.net/3/43/2010/, 2010.

Emmons, L. K., Arnold, S. R., Monks, S. A., Huijnen, V., Tilmes, S., Law, K. S., Thomas, J. L., Raut, J.-C., Bouarar, I., Turquety, S., Long, Y., Duncan, B., Steenrod, S., Strode, S., Flemming, J., Mao, J., Langner, J., Thompson, A. M., Tarasick, D., Apel, E. C., Blake,

D. R., Cohen, R. C., Dibb, J., Diskin, G. S., Fried, A., Hall, S. R., Huey, L. G., Weinheimer, A. J., Wisthaler, A., Mikoviny, T., Nowak, J., Peischl, J., Roberts, J. M., Ryerson, T., Warneke, C., and Helmig, D.: The POLARCAT Model Intercomparison Project (POLMIP): overview and evaluation with observations, Atmospheric Chemistry and Physics, 15, 6721–6744, doi:10.5194/acp-15-6721-2015, http://www.atmos-chem-phys.net/15/6721/2015/, 2015.

Fast, J. D., Gustafson, W. I., Easter, R. C., Zaveri, R. A., Barnard, J. C., Chapman, E. G., Grell, G. A., and Peckham, S. E.: Evolution of ozone, particulates, and aerosol direct radiative forcing in the vicinity of Houston using a fully coupled meteorology-chemistry-aerosol model, Journal of Geophysical Research: Atmospheres, 111, doi:10.1029/2005JD006721, http://dx.doi.org/10.1029/2005JD006721, d21305, 2006.

Grell, G. A., Peckham, S. E., Schmitz, R., McKeen, S. A., Frost, G., Skamarock, W. C., and Eder, B.: Fully coupled "online" chemistry within the WRF model, Atmospheric Environment, 39, 6957–6975, doi:http://dx.doi.org/10.1016/j.atmosenv.2005.04.027, http://www.sciencedirect.com/science/article/pii/S1352231005003560, 2005.

Guenther, A., Karl, T., Harley, P., Wiedinmyer, C., Palmer, P. I., and Geron, C.: Estimates of global terrestrial isoprene emissions using MEGAN (Model of Emissions of Gases and Aerosols from Nature), Atmospheric Chemistry and Physics, 6, 3181–3210, doi:10.5194/acp-6-3181-2006, http://www.atmos-chem-phys.net/6/3181/2006/, 2006.

Huang, L., Gong, S. L., Jia, C. Q., and Lavoué, D.: Importance of deposition processes in simulating the seasonality of the Arctic black carbon aerosol, Journal of Geophysical Research: Atmospheres, 115, doi:10.1029/2009JD013478, http://dx.doi.org/10.1029/2009JD013478, d17207, 2010.

Iacono, M. J., Delamere, J. S., Mlawer, E. J., Shephard, M. W., Clough, S. A., and Collins, W. D.: Radiative forcing by long-lived greenhouse gases: Calculations with the AER radiative transfer models, Journal of Geophysical Research: Atmospheres, 113, doi:10.1029/2008JD009944, http://dx.doi.org/10.1029/2008JD009944, d13103, 2008.

IPCC: Climate Change 2013: The Physical Science Basis. Contribution of Working Group I to the Fifth Assessment Report of the Intergovernmental Panel on Climate Change, Cambridge University Press, Cambridge, United Kingdom and New York, NY, USA, doi:10.1017/CBO9781107415324, www.climatechange2013.org, 2013.

Jacob, D. J., Wofsy, S. C., Bakwin, P. S., Fan, S.-M., Harriss, R. C., Talbot, R. W., Bradshaw, J. D., Sandholm, S. T., Singh, H. B., Browell, E. V., Gregory, G. L., Sachse, G. W., Shipham, M. C., Blake, D. R., and Fitzjarrald, D. R.: Summertime photochemistry of the troposphere at high northern latitudes, Journal of Geophysical Research: Atmospheres, 97, 16 421–16 431, doi:10.1029/91JD01968, http://dx.doi.org/10.1029/91JD01968, 1992.

Jacob, D. J., Crawford, J. H., Maring, H., Clarke, A. D., Dibb, J. E., Emmons, L. K., Ferrare, R. A., Hostetler, C. A., Russell, P. B., Singh, H. B., Thompson, A. M., Shaw, G. E., McCauley, E., Pederson, J. R., and Fisher, J. A.: The Arctic Research of the Composition of the Troposphere from Aircraft and Satellites (ARCTAS) mission: design, execution, and first results, Atmospheric Chemistry and Physics, 10, 5191–5212, doi:10.5194/acp-10-5191-2010, http://www.atmos-chem-phys.net/10/5191/2010/, 2010.

Janjić, Z. I.: The Step-Mountain Eta Coordinate Model: Further Developments of the Convection, Viscous Sublayer, and Turbulence Closure Schemes, Mon. Wea. Rev., 122, 927–945, doi:10.1175/1520-0493(1994)122<0927:TSMECM>2.0.CO;2, http://dx.doi.org/10.1175/1520-0493(1994)122<0927:TSMECM>2.0.CO;2, 1994.

Kain, J. S.: The Kain-Fritsch Convective Parameterization: An Update, Journal of Applied Meteorology, 43, 170–181, doi:10.1175/1520-0450(2004)043<0170:TKCPAU>2.0.CO;2, http://dx.doi.org/10.1175/1520-0450(2004)043<0170:TKCPAU>2.0.CO;2, 2004.

Kain, J. S. and Fritsch, J. M.: A One-Dimensional Entraining/Detraining Plume Model and Its Application in Convective Parameterization, Journal of the Atmospheric Sciences, 47, 2784–2802, doi:10.1175/1520-0469(1990)047<2784:AODEPM>2.0.CO;2, http://dx.doi.org/10.1175/1520-0469(1990)047<2784:AODEPM>2.0.CO;2, 1990.

Klimont, Z., Kupiainen, K., Heyes, C., Purohit, P., Cofala, J., Rafaj, P., Borken-Kleefeld, J., and Schöpp, W.: Global anthropogenic emissions of particulate matter including black carbon, Atmospheric Chemistry and Physics Discussions, 2016, 1–72, doi:10.5194/acp-2016-880, http://www.atmos-chem-phys-discuss.net/acp-2016-880/, 2016.

Klonecki, A., Hess, P., Emmons, L., Smith, L., Orlando, J., and Blake, D.: Seasonal changes in the transport of pollutants into the Arctic troposphere-model study, Journal of Geophysical Research: Atmospheres, 108, doi:10.1029/2002JD002199, http://dx.doi.org/10.1029/2002JD002199, 8367, 2003.

Koch, D., Schulz, M., Kinne, S., McNaughton, C., Spackman, J. R., Balkanski, Y., Bauer, S., Berntsen, T., Bond, T. C., Boucher, O., Chin, M., Clarke, A., De Luca, N., Dentener, F., Diehl, T., Dubovik, O., Easter, R., Fahey, D. W., Feichter, J., Fillmore, D., Freitag, S., Ghan, S., Ginoux, P., Gong, S., Horowitz, L., Iversen, T., Kirkevåg, A., Klimont, Z., Kondo, Y., Krol, M., Liu, X., Miller, R., Montanaro, V., Moteki, N., Myhre, G., Penner, J. E., Perlwitz, J., Pitari, G., Reddy, S., Sahu, L., Sakamoto, H., Schuster, G., Schwarz, J. P., Seland, Ø., Stier, P., Takegawa, N., Takemura, T., Textor, C., van Aardenne, J. A., and Zhao, Y.: Evaluation of black carbon estimations in global aerosol models, Atmospheric Chemistry and Physics, 9, 9001–9026, doi:10.5194/acp-9-9001-2009, http://www.atmos-chem-phys.net/9/9001/2009/, 2009.

Lana, A., Bell, T. G., Simó, R., Vallina, S. M., Ballabrera-Poy, J., Kettle, A. J., Dachs, J., Bopp, L., Saltzman, E. S., Stefels, J., Johnson, J. E., and Liss, P. S.: An updated climatology of surface dimethlysulfide concentrations and emission fluxes in the global ocean, Global Biogeochemical Cycles, 25, doi:10.1029/2010GB003850, http://dx.doi.org/10.1029/2010GB003850, gB1004, 2011.

Law, K. S., Stohl, A., Quinn, P. K., Brock, C. A., Burkhart, J. F., Paris, J.-D., Ancellet, G., Singh, H. B., Roiger, A., Schlager, H., Dibb, J., Jacob, D. J., Arnold, S. R., Pelon, J., and Thomas, J. L.: Arctic Air Pollution: New Insights from POLARCAT-IPY, Bull. Amer. Meteor. Soc., 95, 1873–1895, doi:10.1175/BAMS-D-13-00017.1, http://dx.doi.org/10.1175/BAMS-D-13-00017.1, 2014.

Lelieveld, J. and Crutzen, P. J.: Role of Deep Cloud Convection in the Ozone Budget of the Troposphere, Science, 264, 1759–1761, doi:10.1126/science.264.5166.1759, http://science.sciencemag.org/content/264/5166/1759, 1994.

Li, S.-M. and Barrie, L. A.: Biogenic sulfur aerosol in the Arctic troposphere: 1. Contributions to total sulfate, Journal of Geophysical Research: Atmospheres, 98, 20 613–20 622, doi:10.1029/93JD02234, http://dx.doi.org/10.1029/93JD02234, 1993.

Liu, S. C. and Trainer, M.: Responses of the tropospheric ozone and odd hydrogen radicals to column ozone change, Journal of Atmospheric Chemistry, 6, 221–233, http://dx.doi.org/10.1007/BF00053857, 1988.

Liu, X., Easter, R. C., Ghan, S. J., Zaveri, R., Rasch, P., Shi, X., Lamarque, J.-F., Gettelman, A., Morrison, H., Vitt, F., Conley, A., Park, S., Neale, R., Hannay, C., Ekman, A. M. L., Hess, P., Mahowald, N., Collins, W., Iacono, M. J., Bretherton, C. S., Flanner, M. G., and Mitchell, D.: Toward a minimal representation of aerosols in climate models: description and evaluation in the Community Atmosphere Model CAM5, Geoscientific Model Development, 5, 709–739, doi:10.5194/gmd-5-709-2012, http://www.geosci-model-dev.net/5/709/2012/, 2012.

Ma, P.-L., Rasch, P. J., Wang, H., Zhang, K., Easter, R. C., Tilmes, S., Fast, J. D., Liu, X., Yoon, J.-H., and Lamarque, J.-F.: The role of circulation features on black carbon transport into the Arctic in the Community Atmosphere Model version 5 (CAM5), Journal of Geophysical Research: Atmospheres, 118, 4657–4669, doi:10.1002/jgrd.50411, http://dx.doi.org/10.1002/jgrd.50411, 2013.

Ma, P.-L., Rasch, P. J., Fast, J. D., Easter, R. C., Gustafson Jr., W. I., Liu, X., Ghan, S. J., and Singh, B.: Assessing the CAM5 physics suite in the WRF-Chem model: implementation, resolution sensitivity, and a first evaluation for a regional case study, Geoscientific Model Development, 7, 755–778, doi:10.5194/gmd-7-755-2014, http://www.geosci-model-dev.net/7/755/2014/, 2014.

Mahmood, R., von Salzen, K., Flanner, M., Sand, M., Langner, J., Wang, H., and Huang, L.: Seasonality of global and Arctic black carbon processes in the Arctic Monitoring and Assessment Programme models, Journal of Geophysical Research: Atmospheres, 121, 7100–7116, doi:10.1002/2016JD024849, http://dx.doi.org/10.1002/2016JD024849, 2016JD024849, 2016.

Marelle, L., Raut, J.-C., Thomas, J. L., Law, K. S., Quennehen, B., Ancellet, G., Pelon, J., Schwarzenboeck, A., and Fast, J. D.: Transport of anthropogenic and biomass burning aerosols from Europe to the Arctic during spring 2008, Atmospheric Chemistry and Physics, 15, 3831–3850, doi:10.5194/acp-15-3831-2015, http://www.atmos-chem-phys.net/15/3831/2015/, 2015.

Marelle, L., Thomas, J. L., Raut, J.-C., Law, K. S., Jalkanen, J.-P., Johansson, L., Roiger, A., Schlager, H., Kim, J., Reiter, A., and Weinzierl, B.: Air quality and radiative impacts of Arctic shipping emissions in the summertime in northern Norway: from the local to the regional scale, Atmospheric Chemistry and Physics, 16, 2359–2379, doi:10.5194/acp-16-2359-2016, http://www.atmos-chem-phys.net/16/2359/2016/, 2016.

Matsui, H., Kondo, Y., Moteki, N., Takegawa, N., Sahu, L. K., Zhao, Y., Fuelberg, H. E., Sessions, W. R., Diskin, G., Blake, D. R., Wisthaler, A., and Koike, M.: Seasonal variation of the transport of black carbon aerosol from the Asian continent to the Arctic during the ARCTAS aircraft campaign, Journal of Geophysical Research: Atmospheres, 116, n/a–n/a, doi:10.1029/2010JD015067, http://dx.doi.org/10.1029/2010JD015067, d05202, 2011.

Mölders, N., Porter, S. E., Cahill, C. F., and Grell, G. A.: Influence of ship emissions on air quality and input of contaminants in southern Alaska National Parks and Wilderness Areas during the 2006 tourist season, Atmospheric Environment, 44, 1400–1413, doi:http://dx.doi.org/10.1016/j.atmosenv.2010.02.003, http://www.sciencedirect.com/science/article/pii/S1352231010001044, 2010.

Monks, S. A., Arnold, S. R., Emmons, L. K., Law, K. S., Turquety, S., Duncan, B. N., Flemming, J., Huijnen, V., Tilmes, S., Langner, J., Mao, J., Long, Y., Thomas, J. L., Steenrod, S. D., Raut, J. C., Wilson, C., Chipperfield, M. P., Diskin, G. S., Weinheimer, A., Schlager, H., and Ancellet, G.: Multi-model study of chemical and physical controls on transport of anthropogenic and biomass burning pollution to the Arctic, Atmospheric Chemistry and Physics, 15, 3575–3603, doi:10.5194/acp-15-3575-2015, http://www.atmos-chem-phys.net/15/3575/2015/, 2015.

Morrison, H., Thompson, G., and Tatarskii, V.: Impact of Cloud Microphysics on the Development of Trailing Stratiform Precipitation in a Simulated Squall Line: Comparison of One- and Two-Moment Schemes, Mon. Wea. Rev., 137, 991–1007, doi:10.1175/2008MWR2556.1, http://dx.doi.org/10.1175/2008MWR2556.1, 2009.

Nightingale, P. D., Malin, G., Law, C. S., Watson, A. J., Liss, P. S., Liddicoat, M. I., Boutin, J., and Upstill-Goddard, R. C.: In situ evaluation of air-sea gas exchange parameterizations using novel conservative and volatile tracers, Global Biogeochemical Cycles, 14, 373–387, doi:10.1029/1999GB900091, http://dx.doi.org/10.1029/1999GB900091, 2000.

Quinn, P. K., Shaw, G., Andrews, E., Dutton, E. G., T., R.-A., and Gong, S. L.: Arctic haze: current trends and knowledge gaps, Tellus B, 59, 99–114, doi:10.1111/j.1600-0889.2006.00238.x, http://dx.doi.org/10.1111/j.1600-0889.2006.00238.x, 2007.

Rahn, K. A.: Arctic Air Chemistry Proceedings of the Second Symposium Relative importances of North America and Eurasia as sources of arctic aerosol, Atmospheric Environment (1967), 15, 1447–1455, doi:http://dx.doi.org/10.1016/0004-6981(81)90351-6, http://www.sciencedirect.com/science/article/pii/0004698181903516, 1981.

Raut, J.-C., Marelle, L., Fast, J. D., Thomas, J. L., Weinzierl, B., Law, K. S., Berg, L. K., Roiger, A., Easter, R. C., Heimerl, K., Onishi, T., Delanoë, J., and Schlager, H.: Cross-polar transport and scavenging of Siberian aerosols containing black carbon during the 2012

ACCESS summer campaign, Atmospheric Chemistry and Physics Discussions, 2017, 1–41, doi:10.5194/acp-2016-1023, http://www.atmos-chem-phys-discuss.net/acp-2016-1023/, 2017.

Riahi, K., Rao, S., Krey, V., Cho, C., Chirkov, V., Fischer, G., Kindermann, G., Nakicenovic, N., and Rafaj, P.: RCP 8.5—A scenario of comparatively high greenhouse gas emissions, Climatic Change, 109, 33–57, doi:10.1007/s10584-011-0149-y, http://dx.doi.org/10.1007/s10584-011-0149-y, 2011.

Robinson, A. L., Donahue, N. M., Shrivastava, M. K., Weitkamp, E. A., Sage, A. M., Grieshop, A. P., Lane, T. E., Pierce, J. R., and Pandis, S. N.: Rethinking Organic Aerosols: Semivolatile Emissions and Photochemical Aging, Science, 315, 1259–1262, doi:10.1126/science.1133061, http://science.sciencemag.org/content/315/5816/1259, 2007.

Saltzman, E. S., King, D. B., Holmen, K., and Leck, C.: Experimental determination of the diffusion coefficient of dimethylsulfide in water, Journal of Geophysical Research: Oceans, 98, 16 481–16 486, doi:10.1029/93JC01858, http://dx.doi.org/10.1029/93JC01858, 1993.

Sato, Y., Miura, H., Yashiro, H., Goto, D., Takemura, T., Tomita, H., and Nakajima, T.: Unrealistically pristine air in the Arctic produced by current global scale models, Scientific Reports, 6, 26 561–, http://www.ncbi.nlm.nih.gov/pmc/articles/PMC4879630/, 2016.

Schwarz, J. P., Spackman, J. R., Gao, R. S., Watts, L. A., Stier, P., Schulz, M., Davis, S. M., Wofsy, S. C., and Fahey, D. W.: Global-scale black carbon profiles observed in the remote atmosphere and compared to models, Geophysical Research Letters, 37, doi:10.1029/2010GL044372, http://dx.doi.org/10.1029/2010GL044372, l18812, 2010.

Schwarz, J. P., Weinzierl, B., Samset, B. H., Dollner, M., Heimerl, K., Markovic, M. Z., Perring, A. E., and Ziemba, L.: Aircraft measurements of black carbon vertical profiles show upper tropospheric variability and stability, Geophysical Research Letters, 44, 1132–1140, doi:10.1002/2016GL071241, http://dx.doi.org/10.1002/2016GL071241, 2016GL071241, 2017.

Sessions, W. R., Fuelberg, H. E., Kahn, R. A., and Winker, D. M.: An investigation of methods for injecting emissions from boreal wildfires using WRF-Chem during ARCTAS, Atmospheric Chemistry and Physics, 11, 5719–5744, doi:10.5194/acp-11-5719-2011, http://www.atmos-chem-phys.net/11/5719/2011/, 2011.

Shindell, D., Faluvegi, G., Lacis, A., Hansen, J., Ruedy, R., and Aguilar, E.: Role of tropospheric ozone increases in 20th-century climate change, Journal of Geophysical Research: Atmospheres, 111, doi:10.1029/2005JD006348, http://dx.doi.org/10.1029/2005JD006348, d08302, 2006.

Shindell, D. T., Chin, M., Dentener, F., Doherty, R. M., Faluvegi, G., Fiore, A. M., Hess, P., Koch, D. M., MacKenzie, I. A., Sanderson, M. G., Schultz, M. G., Schulz, M., Stevenson, D. S., Teich, H., Textor, C., Wild, O., Bergmann, D. J., Bey, I., Bian, H., Cuvelier, C., Duncan, B. N., Folberth, G., Horowitz, L. W., Jonson, J., Kaminski, J. W., Marmer, E., Park, R., Pringle, K. J., Schroeder, S., Szopa, S., Takemura, T., Zeng, G., Keating, T. J., and Zuber, A.: A multi-model assessment of pollution transport to the Arctic, Atmospheric Chemistry and Physics, 8, 5353–5372, doi:10.5194/acp-8-5353-2008, http://www.atmos-chem-phys.net/8/5353/2008/, 2008.

Shrivastava, M., Fast, J., Easter, R., Gustafson Jr., W. I., Zaveri, R. A., Jimenez, J. L., Saide, P., and Hodzic, A.: Modeling organic aerosols in a megacity: comparison of simple and complex representations of the volatility basis set approach, Atmospheric Chemistry and Physics, 11, 6639–6662, doi:10.5194/acp-11-6639-2011, http://www.atmos-chem-phys.net/11/6639/2011/, 2011.

Simpson, W. R., von Glasow, R., Riedel, K., Anderson, P., Ariya, P., Bottenheim, J., Burrows, J., Carpenter, L. J., Frieß, U., Goodsite, M. E., Heard, D., Hutterli, M., Jacobi, H.-W., Kaleschke, L., Neff, B., Plane, J., Platt, U., Richter, A., Roscoe, H., Sander, R., Shepson, P., Sodeau, J., Steffen, A., Wagner, T., and Wolff, E.: Halogens and their role in polar boundary-layer ozone depletion, Atmospheric Chemistry and Physics, 7, 4375–4418, doi:10.5194/acp-7-4375-2007, http://www.atmos-chem-phys.net/7/4375/2007/, 2007.

Skamarock, W. C., Klemp, J., Dudhia, J., Gill, D., Barker, D., Duda, M., Huang, X., Wang, W., and Powers., J.: A description of the Advanced Research WRF Version 3, Tech. rep., NCAR, 2008.

Stohl, A.: Characteristics of atmospheric transport into the Arctic troposphere, Journal of Geophysical Research: Atmospheres, 111, doi:10.1029/2005JD006888, http://dx.doi.org/10.1029/2005JD006888, d11306, 2006.

Stohl, A., Klimont, Z., Eckhardt, S., Kupiainen, K., Shevchenko, V. P., Kopeikin, V. M., and Novigatsky, A. N.: Black carbon in the Arctic: the underestimated role of gas flaring and residential combustion emissions, Atmospheric Chemistry and Physics, 13, 8833–8855, doi:10.5194/acp-13-8833-2013, http://www.atmos-chem-phys.net/13/8833/2013/, 2013.

Stohl, A., Aamaas, B., Amann, M., Baker, L. H., Bellouin, N., Berntsen, T. K., Boucher, O., Cherian, R., Collins, W., Daskalakis, N., Dusinska, M., Eckhardt, S., Fuglestvedt, J. S., Harju, M., Heyes, C., Hodnebrog, Ø., Hao, J., Im, U., Kanakidou, M., Klimont, Z., Kupiainen, K., Law, K. S., Lund, M. T., Maas, R., MacIntosh, C. R., Myhre, G., Myriokefalitakis, S., Olivié, D., Quaas, J., Quennehen, B., Raut, J.-C., Rumbold, S. T., Samset, B. H., Schulz, M., Seland, Ø., Shine, K. P., Skeie, R. B., Wang, S., Yttri, K. E., and Zhu, T.: Evaluating the climate and air quality impacts of short-lived pollutants, Atmospheric Chemistry and Physics, 15, 10 529–10 566, doi:10.5194/acp-15-10529-2015, http://www.atmos-chem-phys.net/15/10529/2015/, 2015.

Tanskanen, A. and Manninen, T.: Effective UV surface albedo of seasonally snow-covered lands, Atmospheric Chemistry and Physics, 7, 2759–2764, doi:10.5194/acp-7-2759-2007, http://www.atmos-chem-phys.net/7/2759/2007/, 2007.

Tegen, I. and Fung, I.: Modeling of mineral dust in the atmosphere: Sources, transport, and optical thickness, Journal of Geophysical Research: Atmospheres, 99, 22 897–22 914, doi:10.1029/94JD01928, http://dx.doi.org/10.1029/94JD01928, 1994.

Thomas, J. L., Raut, J.-C., Law, K. S., Marelle, L., Ancellet, G., Ravetta, F., Fast, J. D., Pfister, G., Emmons, L. K., Diskin, G. S., Weinheimer, A., Roiger, A., and Schlager, H.: Pollution transport from North America to Greenland during summer 2008, Atmospheric Chemistry and Physics, 13, 3825–3848, doi:10.5194/acp-13-3825-2013, http://www.atmos-chem-phys.net/13/3825/2013/, 2013.

Wang, H., Easter, R. C., Rasch, P. J., Wang, M., Liu, X., Ghan, S. J., Qian, Y., Yoon, J.-H., Ma, P.-L., and Vinoj, V.: Sensitivity of remote aerosol distributions to representation of cloud-aerosol interactions in a global climate model, Geoscientific Model Development, 6, 765–782, doi:10.5194/gmd-6-765-2013, http://www.geosci-model-dev.net/6/765/2013/, 2013.

Wang, Q., Jacob, D. J., Spackman, J. R., Perring, A. E., Schwarz, J. P., Moteki, N., Marais, E. A., Ge, C., Wang, J., and Barrett, S. R. H.: Global budget and radiative forcing of black carbon aerosol: Constraints from pole-to-pole (HIPPO) observations across the Pacific, Journal of Geophysical Research: Atmospheres, 119, 195–206, doi:10.1002/2013JD020824, http://dx.doi.org/10.1002/2013JD020824, 2013JD020824, 2014.

Wesely, M.: Parameterization of surface resistances to gaseous dry deposition in regional-scale numerical models, Atmospheric Environment (1967), 23, 1293–1304, doi:http://dx.doi.org/10.1016/0004-6981(89)90153-4, http://www.sciencedirect.com/science/article/pii/0004698189901534, 1989.

Wiedinmyer, C., Yokelson, R. J., and Gullett, B. K.: Global Emissions of Trace Gases, Particulate Matter, and Hazardous Air Pollutants from Open Burning of Domestic Waste, Environmental Science & Technology, 48, 9523–9530, doi:10.1021/es502250z, http://dx.doi.org/10.1021/es502250z, pMID: 25019173, 2014.

Wild, O., Zhu, X., and Prather, M. J.: Fast-J: Accurate Simulation of In- and Below-Cloud Photolysis in Tropospheric Chemical Models, Journal of Atmospheric Chemistry, 37, 245–282, doi:10.1023/A:1006415919030, http://dx.doi.org/10.1023/A:1006415919030, 2000.

Wong, J., Barth, M. C., and Noone, D.: Evaluating a lightning parameterization based on cloud-top height for mesoscale numerical model simulations, Geoscientific Model Development, 6, 429–443, doi:10.5194/gmd-6-429-2013, http://www.geosci-model-dev.net/6/429/2013/, 2013.

Zaveri, R. A., Easter, R. C., Fast, J. D., and Peters, L. K.: Model for Simulating Aerosol Interactions and Chemistry (MOSAIC), Journal of Geophysical Research: Atmospheres, 113, doi:10.1029/2007JD008782, http://dx.doi.org/10.1029/2007JD008782, d13204, 2008.